Building a synthetic mechanosensitive signaling pathway in compartmentalized artificial cells

James W. Hindley[a,b,c,1], Daniela G. Zheleva[a,1], Yuval Elani[a,b,c], Kalypso Charalambous[d], Laura M. C. Barter[a,b], Paula J. Booth[c,e], Charlotte L. Bevan[f], Robert V. Law[a,b], and Oscar Ces[a,b,c,2]

[a]Department of Chemistry, Imperial College London, Molecular Sciences Research Hub, W12 0BZ London, United Kingdom; [b]Institute of Chemical Biology, Imperial College London, Molecular Sciences Research Hub, W12 0BZ London, United Kingdom; [c]FABRICELL, Imperial College London and King's College London, W12 0BZ London, United Kingdom; [d]Department of Bioengineering, Imperial College London, South Kensington, SW7 2AZ London, United Kingdom; [e]Department of Chemistry, King's College London, SE1 1DB London, United Kingdom; and [f]Imperial Centre for Translational and Experimental Medicine, Department of Surgery & Cancer, Imperial College London, Hammersmith Hospital, W12 0NN London, United Kingdom

Edited by David A. Weitz, Harvard University, Cambridge, MA, and approved June 24, 2019 (received for review March 11, 2019)

To date, reconstitution of one of the fundamental methods of cell communication, the signaling pathway, has been unaddressed in the bottom-up construction of artificial cells (ACs). Such developments are needed to increase the functionality and biomimicry of ACs, accelerating their translation and application in biotechnology. Here, we report the construction of a de novo synthetic signaling pathway in microscale nested vesicles. Vesicle-cell models respond to external calcium signals through activation of an intracellular interaction between phospholipase A2 and a mechanosensitive channel present in the internal membranes, triggering content mixing between compartments and controlling cell fluorescence. Emulsion-based approaches to AC construction are therefore shown to be ideal for the quick design and testing of new signaling networks and can readily include synthetic molecules difficult to introduce to biological cells. This work represents a foundation for the engineering of multicompartment-spanning designer pathways that can be utilized to control downstream events inside an AC, leading to the assembly of micromachines capable of sensing and responding to changes in their local environment.

artificial cells | signaling pathway | nested vesicle | MscL | phospholipase A2

To sense and respond to their external environment, biological cells have developed various means of communication (1–3). One of the most fundamental communication strategies in biological systems is to convert an external chemical input into a functional output, primarily through signal transduction. Here, the controlled activation of protein machinery is often used to initiate gene transcription and translation of proteins that result in a functional change in cellular behavior. One ubiquitous signaling molecule is the divalent calcium ion (Ca^{2+}), which is utilized across biology (4), controlling both intracellular and intercellular processes, including transcription (5), mitochondrial energy production (6), and apoptosis (7). Calcium influx occurs across the plasma membrane as well as from intracellular stores in the endoplasmic reticulum, resulting in the activation of signaling cascades involving calcium-dependent enzymes (8, 9).

There is great interest in generating synthetic transduction pathways to control cell function as well as to increase fundamental understanding of cellular behavior (10). Many efforts have focused on the manipulation of existing pathways by creating chimeric proteins that combine the sensing domains of 1 protein with the signaling output of another (11, 12). This strategy has been used to control protein activity through foreign autoinhibitory interactions (11), leading to the downstream control of cell morphology (12), organization (13), and migration (14). More recent work has focused on a generalized approach to controlling transduction, in which a modular extracellular sensor combined with a rewired signaling pathway enables transgene expression (15).

These approaches have used genetic manipulation of existing eukaryotes or prokaryotes. An alternative method for engineering biology comes from the bottom-up construction of biological systems (16, 17). This nascent field aims to create soft-matter structures with cellular functions and behaviors that are engineered to carry out specific tasks. Artificial cells (ACs) can be constructed from biological or synthetic molecules and have been used to reconstitute cellular behaviors such as protein expression (18), cell division (19), and minimal metabolism (20). They are also capable of communication; both AC–AC (21) and AC–biological-cell (22) communication systems have been developed through the combination of sensing modules with cell-free expression outputs. This can enable ACs to behave as chemical translators, allowing nonnatural bacterial communication to occur (22). Exogenous stimuli such as light have also been utilized to control gene expression in synthetic tissues (23), enzymatic microreactors (24, 25), and artificial photosynthetic organelles (26).

One challenge unaddressed to date involves the creation of de novo signaling pathways in bottom-up systems, which is particularly important given the difficulty in reconstituting native transduction pathways involving G protein-coupled receptors (27). Constructing new signaling pathways from the bottom up is needed to alleviate a bottleneck that has hindered the design of ACs with enhanced functionalities—for example, that can dynamically respond to their surroundings through activation of internal processes. The relative simplicity of ACs makes them an ideal foundation for pathway construction; recombinant proteins

Significance

In nature, an external input is translated by cellular machinery into a downstream effect through signaling pathways, enabling cells to respond to their environment. Bottom-up synthetic biology aims to re-create cellular organization and function through the creation of "artificial cells" (ACs) through molecular self-assembly. Although the construction of new signaling pathways will enable increasingly responsive ACs, this area is undeveloped; here, we show that multicompartment lipid vesicles are an ideal framework to build a pathway not found in nature. External calcium ions activate internal protein communication, leading to control of cell fluorescence. This highlights the potential of ACs for design and construction of synthetic pathways difficult to reconstitute in existing cells, leading to development of environment-responsive molecular machines in biotechnology.

Author contributions: J.W.H., Y.E., and O.C. designed research; J.W.H., D.G.Z., Y.E., and K.C. performed research; P.J.B. contributed new reagents/analytic tools; J.W.H., D.G.Z., and Y.E. analyzed data; and J.W.H., Y.E., L.M.C.B., C.L.B., R.V.L., and O.C. wrote the paper

The authors declare no conflict of interest.

This article is a PNAS Direct Submission.

[1]J.W.H. and D.G.Z. contributed equally to this work.

[2]To whom correspondence may be addressed. Email: o.ces@imperial.ac.uk.

This article contains supporting information online at www.pnas.org/lookup/suppl/doi:10.1073/pnas.1903500116/-/DCSupplemental.

Published online August 1, 2019.

can be readily combined with nonnatural sensing (28), structural (29), and processing (30) molecules found in chemistry and nanotechnology to create plug-and-play networks that are challenging to integrate into a living system. Here, we make use of a previously reported interaction in which 1 protein (P1) can interact with a second (P2) using the membrane (M) as a communication pathway (31). This protein–membrane–membrane protein interaction (P1-M-P2) has been used to control triggered release from a population of mechanosensitive vesicles, where P1 and P2 are secretory phospholipase A2 ($sPLA_2$) and the mechanosensitive channel of large conductance (MscL), respectively.

$sPLA_2$ (P1) is a calcium-dependent enzyme that catalyzes phosphatidylcholine lipids to lyso-phosphatidylcholine (LPC) and a concomitant fatty acid at the *sn*-2 position (32). Production of LPC in the external leaflet of vesicles results in an asymmetric change in the lateral pressure profile of the membrane (M) (33). This can be sensed by MscL (P2), a homopentameric integral membrane protein that can respond to changes in membrane mechanics (34, 35) by opening a large, nonspecific pore ∼2.5–3 nm in diameter (36), resulting in content release of molecules up to 10 kDa in size (37). The response of MscL to $sPLA_2$ can be considered as a protein–protein interaction that occurs through the lipid bilayer itself and has the potential to be used as a network motif to couple chemical or mechanical changes within an AC to a functional output.

As the $sPLA_2$–M–MscL network relies on active phospholipase enzymes as an input, in theory, the full network can be activated by the controlled introduction of calcium into the AC. Here, we demonstrate that P1-M-P2 networks can be used to trigger events in a compartmentalized AC, making use of the $sPLA_2$–M–MscL network to control the concentration of the fluorescent molecule calcein in the vesicle lumen (Fig. 1). To do this, we employed a nested vesicle motif (25), where mechanosensitive inner vesicle compartments were encapsulated in a larger vesicle (Fig. 1*A*). This was achieved by combining traditional detergent-mediated protein-reconstitution strategies (38) with emulsion phase transfer (39). The phospholipase enzyme was also encapsulated in the larger vesicle, but was rendered inactive through the inclusion of the calcium chelator ethylenediaminetetraacetic acid (EDTA). An EDTA-saturating calcium flux can be controllably introduced by permeabilizing the outer vesicle membrane with alpha hemolysin (αHL) (40). By increasing the availability of calcium within the AC, the $sPLA_2$–M–MscL network was activated (Fig. 1*B*), and the fluorescence of the AC was increased through calcein release into the main compartment of the vesicle (Fig. 1*C*).

Here, a synthetic signaling pathway has been created in a bottom-up synthetic biological system and represents a foundation for the engineering of multicompartment-spanning designer pathways that can be utilized to control downstream events inside an AC.

Results

Using Nested Vesicle Systems to Build Synthetic Communication Pathways. We have recently shown that functional nested vesicles [otherwise known as vesosomes (41)] can be created by using emulsion phase transfer and lend themselves well to a modular-based construction approach (25). By loading giant vesicles with a mechanosensitive vesicle "module," the feasibility of pathway creation in bottom-up systems can be readily tested.

Making use of the size-independent encapsulation of water-soluble molecular species intrinsic to emulsion phase transfer (42) (*SI Appendix*, Fig. S1), we assembled the nested vesicle system containing an outer lipid membrane composed of 1-palmitoyl-2-oleoyl-*i*-glycero-3-phosphocholine (POPC), which contained 1,2-dioleoyl-*sn*-glycero-3-phophocholine (DOPC) and 1,2-dioleoyl-*sn*-glycero-3-phophoglycerol (DOPG) large unilamellar vesicles (LUVs) at a 1:1 molar ratio containing reconstituted G22C F93W MscL and a self-quenching concentration of calcein. The bee venom phospholipase A2 enzyme and EDTA were also encapsulated. Nested vesicle composition is shown and discussed further in *SI Appendix*, Fig. S2 and Table S1; the stability and functionality of this composition was determined from initial experiments with mechanosensitive vesicles as detailed below and in *SI Appendix*. Gel electrophoresis data of the purified G22C F93W mutant of MscL (*Escherichia coli*) are additionally shown in *SI Appendix*, Fig. S3.

To activate the nested system, permeabilization of the outer membrane is necessary due to the low permeability of Ca^{2+} across lipid bilayers. We achieved this through the addition of αHL, a water-soluble protein toxin that can self-assemble in the membrane to form oligomeric pores that are permanently open (40). Previous work (43) has shown that αHL will readily self-assemble in giant unilamellar vesicle (GUV) membranes, enabling permeation of small molecules. To confirm successful encapsulation of the nested structure of MscL vesicles in the GUV, inner compartments were labeled with Rhodamine–PE lipid to fluorescently visualize the full system. By using bright-field and fluorescence microscopy, the outer membrane, inner membranes, and calcein cargo can be visualized (*SI Appendix*, Fig. S4 *A–C*, respectively), confirming that the nested structure was successfully produced. Confocal fluorescence microscopy was then used to quantify the encapsulation efficiency of inner LUV compartments. The average encapsulation efficiency of PC:PG vesicles at millimolar concentration in POPC GUVs was estimated to be 67.59 ± 1.94% (*SI Appendix*, Table S2), as estimated by using the linear relationship in DOPC:DOPG lipid concentration and Rhodamine–PE fluorescence obtained between concentrations of 0.0225 and 6.35 mM ($r^2 = 0.992$; *SI Appendix*, Fig. S5*A*). This loss is attributed to the rupture of encapsulated vesicles to stabilize the water/oil interface during emulsion generation (44), is acceptable for the proof-of-principle work undertaken here, and is favorable compared with previous methods of nested vesicle production (*SI Appendix*, *Note 1*).

To confirm network activation, fluorescence spectroscopy and microscopy were used to assess calcein fluorescence changes in the full vesicle population, as well as to monitor changes in individual vesicles. As shown in Fig. 1*D* and *SI Appendix*, Fig. S6, nested vesicles containing MscL in their inner-compartment membranes can successfully respond to a calcium concentration of 10 mM, showing ∼10-fold increase in calcein fluorescence 100 min after Ca^{2+} addition, compared with nested vesicles lacking the channel. Lower (2.5 mM) and higher (15 or 30 mM) calcium concentrations resulted in either negligible or MscL-independent release of calcein, respectively; negligible release occurred at low Ca^{2+} concentrations due to insufficient Ca^{2+} present to saturate the EDTA in the vesicle, while at high Ca^{2+} concentrations, MscL-vesicle aggregation within the GUV led to uncontrolled calcein flux, as shown by dynamic light scattering (*SI Appendix*, Fig. S7). This flux could occur due to the high local concentrations of LPC and oleic acid produced upon phospholipase activity of aggregated vesicles, which can act as membrane-permeability enhancers (45). Oleic acid is also known to mediate membrane fusion between calcium-aggregated phosphatidylserine vesicles, where content leakage to the environment occurs alongside fusion (46). Stability of inactivated nested vesicles was additionally monitored (*SI Appendix*, Fig. S8); without permeabilization of the outer membranes with αHL, a slow decrease in fluorescence occurred over 14 h, indicating that negligible calcein leakage was occurring from the inner, mechanosensitive vesicles due to enzyme activation or passive leakage, and the full system was stable.

While fluorescence spectroscopy of the full system indicated that the mechanosensitive pathway could be controlled inside nested vesicles, spectroscopy captures solution fluorescence and so only gives information on the whole vesicle population. As nested vesicles exist on the microscale, fluorescence microscopy can be employed to monitor the fluorescence of individual vesicles (Fig. 1*E*). To confirm that the positive result observed in spectroscopy measurements was due to the controlled activation of the mechanosensitive pathway within the giant vesicle and not caused by the destruction of the nested structure, αHL followed by 10 mM Ca^{2+} was added to a

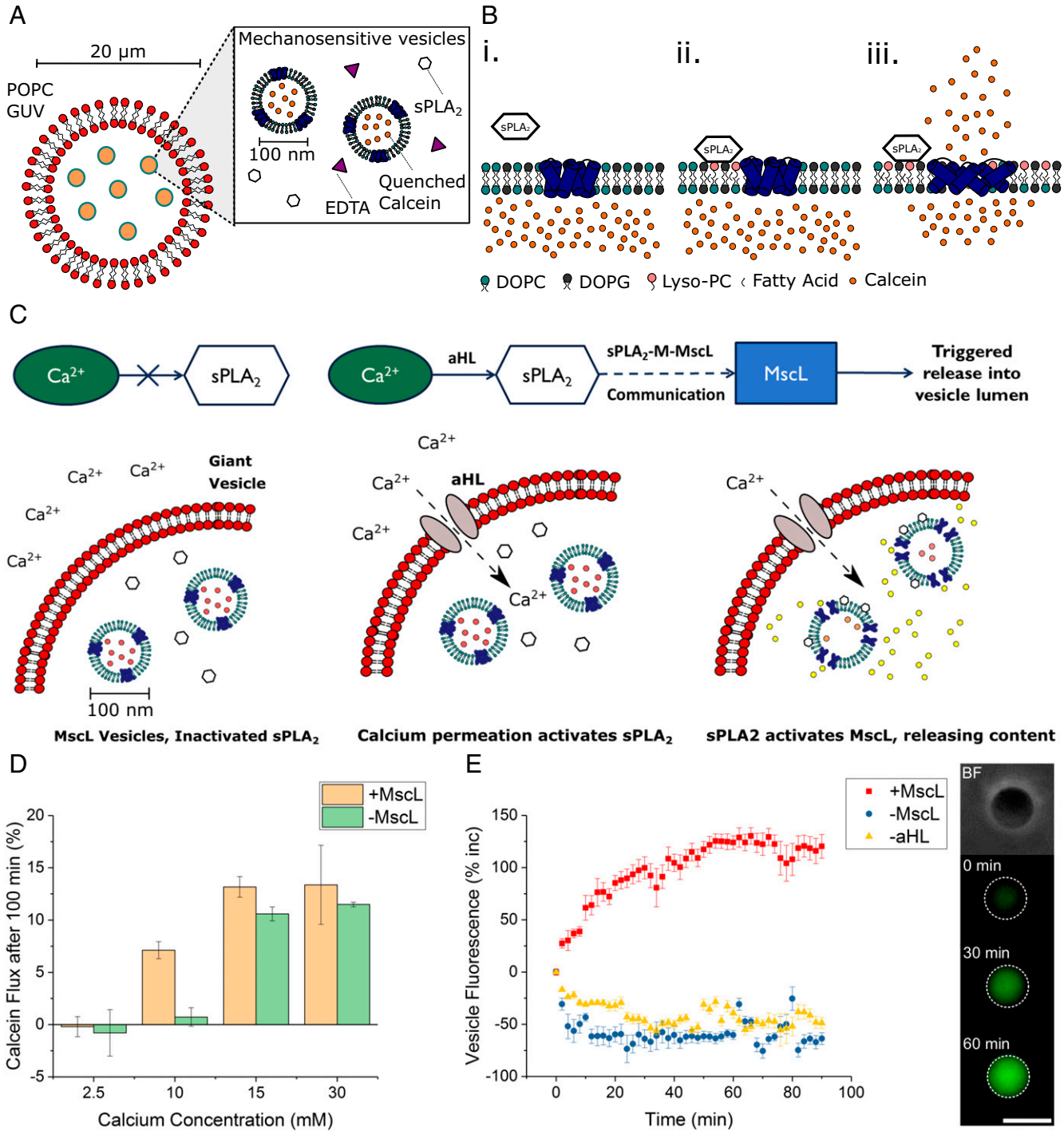

Fig. 1. Using the $sPLA_2$–M–MscL network to build a synthetic mechanosensitive signaling pathway inside an artificial cell (AC). (*A*) Composition of the nested AC: A microscale POPC membrane encloses 1:1 DOPC:DOPG vesicles containing reconstituted mechanosensitive channel of large conductance (MscL), secretory phospholipase A2 ($sPLA_2$) enzyme, and EDTA to chelate trace calcium present in the AC. (*B*) Function of the $sPLA_2$–M–MscL network. (*B*, *i*) MscL is reconstituted into a DOPC:DOPG membrane and is closed in the absence of tension or asymmetry in the membrane. $sPLA_2$ is added to the solution. (*B*, *ii*) $sPLA_2$ binds to the membrane and begins to catalyze the production of LPC and a concomitant fatty acid. The asymmetric generation of LPC begins to asymmetrically change the pressure profile of the lipid bilayer. (*B*, *iii*) Once a critical amount of LPC has been produced, MscL responds to the lateral pressure change by opening to form a 3- to 4-nm diameter pore in the lipid bilayer, releasing encapsulated cargo across the membrane. (*C*) Proposed functioning of the synthetic mechanosensitive signaling pathway. Ca^{2+} is prevented from entering the nested vesicle due to the presence of the outer POPC membrane. Permeabilization of the outer membrane (here accomplished with αHL) then results in a calcium influx, activating latent $sPLA_2$ in the vesicle lumen. This activates the $sPLA_2$–M–MscL network, resulting in content release (and potentially the control of downstream events) within the AC. (*D*) Monitoring activation of the mechanosensitive pathway with fluorescence spectroscopy. Successful activation is triggered by the addition of ∼10 mM Ca^{2+}. Error bars represent 1 SD ($n = 3$). (*E*) Confirming activation of the pathway through fluorescence microscopy of individual nested vesicles. (*E*, *Left*) Both MscL and αHL are necessary to increase vesicle fluorescence (red squares), while absence of MscL (blue circles) or αHL (yellow triangles) prevents network activation. Error bars represent 1 SEM ($n = 15$, 14, and 13, respectively). *E*, *Right* highlights micrographs of a nested vesicle in bright-field and fluorescence microscopy of pathway activation within the nested vesicle at $t = 0$, 30, and 60 min, respectively. (Scale bar, 10 μm.)

population of nested vesicles before monitoring individual vesicle fluorescence over 90 min. As shown in Fig. 1*E*, if MscL was present in the internal membranes, a fluorescence-intensity increase could be observed in the vesicles (red squares). If, however, either MscL was absent from the internal membranes (blue circles) or αHL from the external membrane (yellow triangles), no increase in fluorescence occurred. The gradual overall decrease over time for control experiments is attributed to photobleaching of calcein in the inactivated systems.

Statistical testing confirmed that the fluorescence increases for vesicles containing the full pathway was significant compared with both the –MscL and –αHL controls ($P < 0.005$; unpaired t test, $n = 15$, 14, and 13 for full system, –MscL, and –αHL, respectively). Interestingly, we note that the release behavior observed in nested vesicles is comparable to calcein release from unencapsulated mechanosensitive vesicles activated with $sPLA_2$ (Fig. 2*A*). As the time constants from the fitted exponential functions are within error ($t1_{nested} = 19.61 \pm 1.36$ min, $t1_{free} = 18.83 \pm 0.58$ min), we conclude that the release rate of calcein in the nested system is equivalent to calcein release profiles from free vesicles (*SI Appendix*, *Note 2* and Fig. S9). This confirms that the pathway is functional, that both proteins are necessary for pathway activity, and that bulk release behavior has been successfully compartmentalized. Additionally, the lack of activity in the absence of MscL confirms that nested vesicle fluorescence increase is not due to permeabilization of inner membranes by αHL, indicating that these results are a true reflection of pathway functionality. We can therefore attribute the increase in fluorescence observed in spectroscopy experiments to a controlled activation of the pathway inside the microcompartment of the nested vesicle.

Controlling $sPLA_2$–M–MscL Network Activity via Calcium Chelation. Before encapsulation of the full system was attempted, it was critical to confirm that $sPLA_2$–M–MscL network function could be controlled through calcium chelation. Large unilamellar DOPC:DOPG vesicles were produced through thin-film rehydration, extrusion, and detergent-mediated reconstitution of recombinant G22C F93W MscL. After removing octyl β-D-glucopyranoside detergent from vesicles by using hydrophobic adsorption chromatography, unencapsulated calcein was removed through size-exclusion chromatography (*SI Appendix*, Fig. S10) to yield calcein-loaded MscL vesicles ∼100 nm in diameter (*SI Appendix*, Fig. S11).

Network function was demonstrated through the $sPLA_2$-dependent release of calcein from MscL-containing vesicles (Fig. 2). Here, concentration dependence was observed over 3 orders of magnitude from 0.05 to 5.00 nM (0.3–30 U/mL) for vesicles containing MscL. If the channel was removed from the membrane, negligible release was observed over 100 min, indicating that MscL is key to triggering calcein flux from DOPC:DOPG vesicles at the low concentrations of $sPLA_2$ used here.

After confirming network function, the next step was to successfully inactivate $sPLA_2$. EDTA is a hexadentate ligand which chelates divalent cations and removes them from solution, and, as such, increasing concentrations of the calcium chelator EDTA were added to MscL vesicles (Fig. 3*A*). The observed calcein flux 1 h after the addition of 0.5 nM $sPLA_2$ was then used as a measure to estimate the fraction of Ca^{2+} chelation in solution. An EDTA-dependent reduction in calcein flux was observed with increasing EDTA concentration, with leakage significantly reduced upon addition of 0.25 mM EDTA before being reduced to background levels from 0.5 mM EDTA and upward. It can therefore be inferred that 2.5-fold to 5-fold greater EDTA is necessary to fully chelate 0.1 mM Ca^{2+}. This is likely due to competition for calcium association by the strongly negatively charged MscL vesicles (47), as well as the pentachelating state of EDTA at pH 7.4, which reduces the affinity of the molecule for Ca^{2+} (48).

Once network inhibition was successfully shown, reactivation of the network through addition of Ca^{2+} to systems inhibited with 2.5 mM EDTA was undertaken. Here, calcein flux of the system was measured for 45 min to confirm that complete inhibition was occurring (*SI Appendix*, Fig. S12). Different concentrations of Ca^{2+} (0.5–10.0 mM) were then introduced into solution, and fluorescence was monitored for a further 90 min, as shown in Fig. 3*B*. As expected, addition of upward of 2.5 mM Ca^{2+} caused reactivation of the network, resulting in Ca^{2+} concentration-dependent calcein flux from vesicles 60 min after Ca^{2+} addition (Fig. 3*C*). Again, if the MscL channel was removed from vesicles, concentration-dependent flux was lost, indicating that the channel is essential for triggered release.

Discussion

In this work, we demonstrate the creation of a nested vesicle-in-vesicle AC that can respond to an external Ca^{2+} stimulus by initiating a mechanosensitive $sPLA_2$–M–MscL network, which

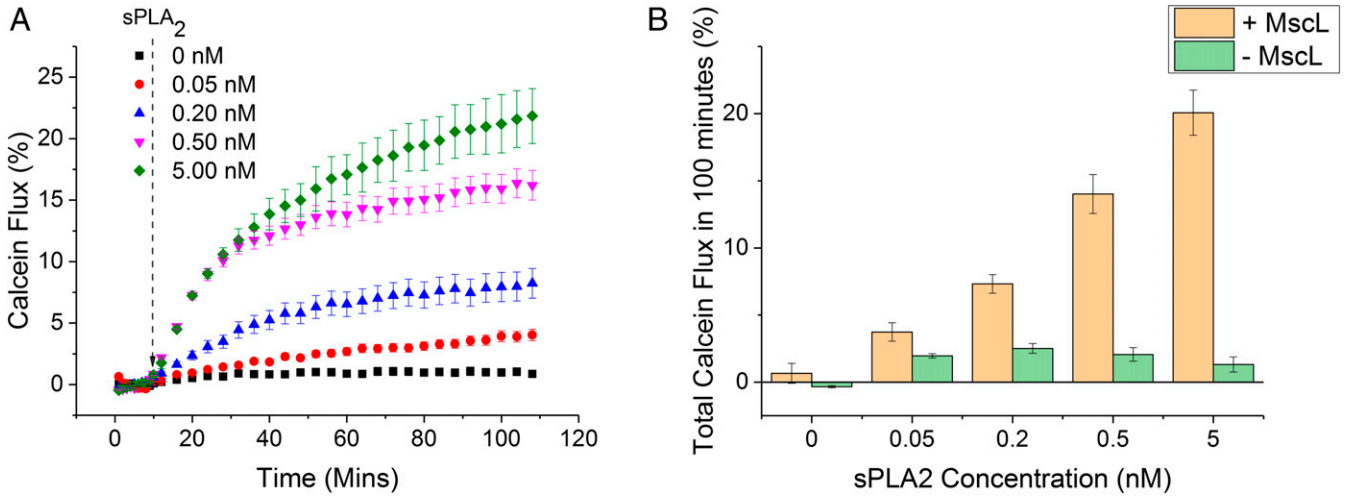

Fig. 2. MscL is essential for $sPLA_2$–M–MscL communication. (*A*) The release of calcein from 1:1 DOPC:DOPG vesicles can be monitored spectroscopically over time. $sPLA_2$ is added at 10 min, before monitoring calcein fluorescence for 100 min. Release of calcein from vesicles results in a fluorescence increase as the dye dilutes in external solution and self-quenching becomes inefficient. Error bars show propagated error of 1 SD ($n = 3$). (*B*) Total calcein flux at 100 min for vesicles ± MscL. $sPLA_2$-concentration-dependent calcein flux is only observed for vesicles containing MscL. Error bars show 1 SD ($n = 3$).

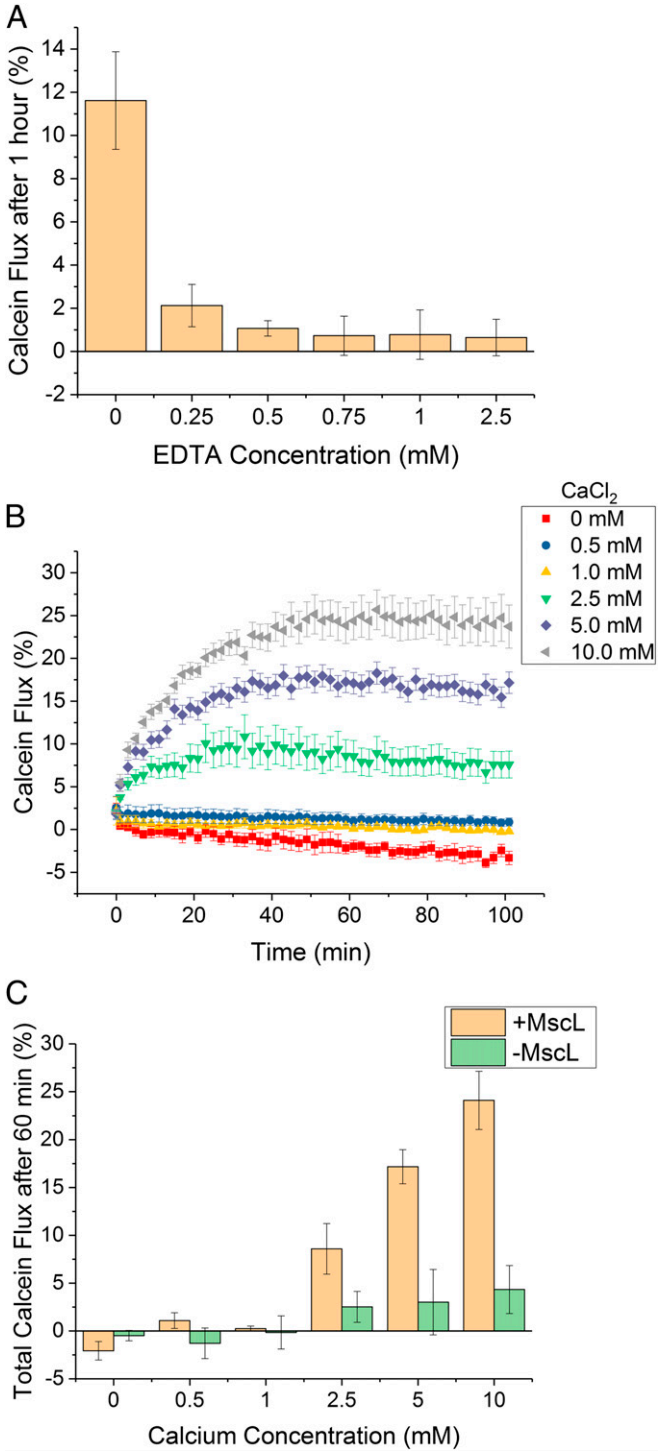

Fig. 3. The $sPLA_2$–M–MscL network can be controlled through calcium chelation. (*A*) $sPLA_2$ inactivation, and hence network activation, can be achieved through the addition of increasing concentrations of the Ca^{2+} chelator EDTA. Error bars = 1 SD (n = 3). (*B*) Monitoring reactivation of the network using calcein flux after the addition of Ca^{2+} (0–10.0 mM) to solutions containing the network and 2.5 mM EDTA. Error bars show 1 SD (n = 3). (*C*) Total calcein flux after 60 min for 1:1 DOPC:DOPG vesicles ± MscL showing that the MscL channel is necessary for network reactivation with Ca^{2+}. Error bars show 1 SD (n = 3).

results in controlled calcein release from nanoscale MscL vesicles into the main compartment of the AC. Similarities between the engineered pathway and that of biological transduction processes include: the use of a Ca^{2+} as a key messenger in the process; the ∼20,000-fold increase in calcium concentration (nanomolar to millimolar) in the AC lumen upon pathway activation (5); the controlled activation of protein machinery in the pathway; and a resultant change in the cell (in our case, simply in its temporal fluorescent behavior). This pathway acts as a foundation that can be extended in 2 main ways:

1) Integrating the use of a primary messenger to gate calcium flux into the AC (resulting in signal amplification).
2) Enabling a biochemical output for the pathway.

The first point can be addressed through reconstitution of receptor proteins—for example, glutamate receptors from the excitatory neurotransmitter pathway which respond to a glutamate primary messenger by triggering calcium influx (49). However, one of the major advantages when designing bottom-up synthetic biology structures is that elements of extant biological machinery can be combined with nonnative molecular systems. This enables a streamlining of pathway design that can result in the construction of synthetic pathways with equivalent functional output, but that are simpler in design to transduction pathways created by nature.

In this proof-of-principle study, we have utilized αHL to solve the problem of controlled calcium introduction to the AC. This paves the way for the development of second-generation systems, utilizing rational design of the cell structure to modulate membrane permeability. Although only fluorescence changes within the AC have been produced as the output in this work, more complex molecular processes can be controlled through triggered-release strategies. As MscL has a large pore diameter of ∼2.5–3 nm when open, small molecules, biopolymers, and even small proteins can pass through the channel (37). This, coupled with the use of emulsion phase transfer to create the nested vesicles, gives versatility when considering pathway design, as size-independent content encapsulation can be achieved alongside the system developed here. As such, further complexity can be readily built into the designed system, opening up the possibility for the creation of multiresponsive ACs. Future work will focus on extending the pathway as well as building reversibility into the $sPLA_2$–M–MscL interaction utilized here.

In conclusion, we have designed a multicompartment, synthetic communication pathway that utilizes protein communication through inner lipid membranes to control the fluorescence behavior of an AC. The framework designed here is modular and can be readily integrated with the increasingly large toolkit offered by bottom-up synthetic biology to create a new generation of ACs. These structures can be quickly designed and tested compared with the genetic editing of extant biological systems, persist for shorter lengths of time in the environment, and be rationally designed to utilize all available resources to accomplish their primary function. Such soft-matter systems could be utilized across biotechnology, functioning as responsive biochemical factories that could be applied in areas from environmental remediation to the long-term monitoring of disease development in vivo.

Materials and Methods

Expression and Purification of Recombinant G22C F93W MscL. *E. coli* BL21 (DE3) cells carrying the chemically gated MscL gene (G22C, F93W) grown overnight in Luria broth (LB) were reseeded 1:100 into 1 L of fresh LB (30 μg/mL kanamycin) and incubated at 37 °C and 250 rpm to the maximum of the exponential phase (OD_{600} = 1). Expressed MscL was then solubilized by using dodecyl maltoside (DDM; 2 wt/vol%) in buffer before pelleting the insoluble fraction and purifying solubilized MscL with cobalt metal-affinity chromatography. Purified protein was then desalted before concentrating to 0.15–1.5 mM concentration of MscL pentamer. See *SI Appendix* for full experimental methods.

Preparation of 1:1 DOPC:DOPG LUVs Containing Reconstituted MscL. A 1:1 DOPC:DOPG (mol/mol) film was rehydrated with 40 mM octyl-β-D-glucopyranoside, 50 mM calcein, 20 mM Hepes, and 100 mM KCl at pH 7.4 at 10 mg/mL lipid concentration before freeze-thawing 3 times and extruding the resultant

suspension 11 times with a 100-nm filter. Vesicles were then incubated with MscL at a 50,000:1 lipid:protein molar ratio before removing detergent with 3 × 100 mg of SM-2 Bio-Beads. Vesicles were then purified by using size-exclusion chromatography. Controls lacking MscL were prepared identically, except with the addition of 0.13% DDM. See *SI Appendix* for full experimental methods.

Formation of Nested Vesicles via Emulsion Phase Transfer. POPC was suspended in mineral oil at a concentration of 2 mg/mL. Emulsions were then generated at 10:1 (vol/vol) POPC in mineral oil by mixing POPC-in-oil with an aqueous phase containing MscL vesicles, $sPLA_2$, and EDTA. The emulsion was then layered on top of an equimolar glucose buffer before centrifuging the sample to form a nested vesicle pellet. Oil and glucose were then removed before resuspending the nested vesicles in fresh glucose buffer, and this cycle was repeated. See *SI Appendix* for full experimental methods.

Fluorescence Spectroscopy of Vesicles. Calcein fluorescence was recorded at $\lambda_{ex/em}$ = 494/514 nm. LUVs ± MscL were diluted in sucrose buffer at a 1:50 (vol/vol) ratio, while nested vesicles ± MscL were diluted in sucrose buffer at a 1:8 (vol/vol) ratio. Baseline recordings (F_0) were collected for 10+ min before reagent addition in all experiments. Triton X-100 (3% vol/vol) was added at the end of each assay to enable complete vesicle lysis (F_{END}) and data normalization. See *SI Appendix* for full experimental methods and data analysis.

Optical and Fluorescence Microscopy of Vesicles. GUVs were imaged on a Nikon Eclipse TE 2000-E Inverted Microscope connected to a QICAM camera (QImaging) illuminated by a mercury arc lamp. The TRITC filter [excitation (Ex.) 535 nm, emission (Em.) 590 nm, dichroic 575 nm] and the FITC filter (Ex. 489 nm, Em. 535 nm, dichroic 505 nm) were used to capture rhodamine and calcein fluorescence, respectively. Phase-contrast and fluorescence images were taken of all samples. All images were analyzed and manipulated by using ImageJ software (National Institutes of Health). Fluorescence intensity was extracted by using the Mean Gray Value option. See *SI Appendix* for full experimental methods.

Data and Materials Availability. All data necessary for interpretation of the study is contained between the article and the *SI Appendix*.

ACKNOWLEDGMENTS. This work was supported by an Engineering and Physical Sciences Research Council (EPSRC) Centre for Doctoral Training Studentship from the Institute of Chemical Biology (Imperial College London) (to J.W.H.); EPSRC Fellowship EP/N016998/1 (to Y.E.); and EPSRC Grants EP/J017566/1 and EP/K038648/1 (to O.C.).

1. E. C. Lai, Notch signaling: Control of cell communication and cell fate. *Development* **131**, 965–973 (2004).
2. C. M. Waters, B. L. Bassler, Quorum sensing: Cell-to-cell communication in bacteria. *Annu. Rev. Cell Dev. Biol.* **21**, 319–346 (2005).
3. J. Ratajczak, M. Wysoczynski, F. Hayek, A. Janowska-Wieczorek, M. Z. Ratajczak, Membrane-derived microvesicles: Important and underappreciated mediators of cell-to-cell communication. *Leukemia* **20**, 1487–1495 (2006).
4. H. Rasmussen, Cell communication, calcium ion, and cyclic adenosine monophosphate. *Science* **170**, 404–412 (1970).
5. D. E. Clapham, Calcium signaling. *Cell* **131**, 1047–1058 (2007).
6. A. I. Tarasov, E. J. Griffiths, G. A. Rutter, Regulation of ATP production by mitochondrial Ca^{2+}. *Cell Calcium* **52**, 28–35 (2012).
7. A. Rasola, P. Bernardi, Mitochondrial permeability transition in Ca^{2+}-dependent apoptosis and necrosis. *Cell Calcium* **50**, 222–233 (2011).
8. S. S. Grewal *et al*., Calcium and cAMP signals differentially regulate cAMP-responsive element-binding protein function via a Rap-1-extracellular signal-regulated kinase pathway. *J. Biol. Chem.* **275**, 34433–34441 (2000).
9. J. W. Putney, T. Tomita, Phospholipase C signaling and calcium influx. *Adv. Biol. Regul.* **52**, 152–164 (2012).
10. C. Kiel, E. Yus, L. Serrano, Engineering signal transduction pathways. *Cell* **140**, 33–47 (2010).
11. J. E. Dueber, B. J. Yeh, K. Chak, W. A. Lim, Reprogramming control of an allosteric signaling switch through modular recombination. *Science* **301**, 1904–1908 (2003).
12. B. J. Yeh, R. J. Rutigliano, A. Deb, D. Bar-Sagi, W. A. Lim, Rewiring cellular morphology pathways with synthetic guanine nucleotide exchange factors. *Nature* **447**, 596–600 (2007).
13. S. Toda, L. R. Blauch, S. K. Y. Tang, L. Morsut, W. A. Lim, Programming self-organizing multicellular structures with synthetic cell-cell signaling. *Science* **361**, 156–162 (2018).
14. Y. I. Wu *et al*., A genetically encoded photoactivatable Rac controls the motility of living cells. *Nature* **461**, 104–108 (2009).
15. L. Scheller, T. Strittmatter, D. Fuchs, D. Bojar, M. Fussenegger, Generalized extracellular molecule sensor platform for programming cellular behavior article. *Nat. Chem. Biol.* **14**, 723–729 (2018).
16. J. Szostak, D. Bartel, P. Luisi, Synthesizing life. *Nature* **409**, 387–390 (2001).
17. P. Schwille, Jump-starting life? Fundamental aspects of synthetic biology. *J. Cell Biol.* **210**, 687–690 (2015).
18. V. Noireaux, A. Libchaber, A vesicle bioreactor as a step toward an artificial cell assembly. *Proc. Natl. Acad. Sci. U.S.A.* **101**, 17669–17674 (2004).
19. K. Kurihara *et al*., Self-reproduction of supramolecular giant vesicles combined with the amplification of encapsulated DNA. *Nat. Chem.* **3**, 775–781 (2011).
20. P. M. Gardner, K. Winzer, B. G. Davis, Sugar synthesis in a protocellular model leads to a cell signalling response in bacteria. *Nat. Chem.* **1**, 377–383 (2009).
21. Y. Ding, L. E. Contreras-Llano, E. Morris, M. Mao, C. Tan, Minimizing context dependency of gene networks using artificial cells. *ACS Appl. Mater. Interfaces* **10**, 30137–30146 (2018).
22. R. Lentini *et al*., Two-way chemical communication between artificial and natural cells. *ACS Cent. Sci.* **3**, 117–123 (2017).
23. M. J. Booth, V. R. Schild, A. D. Graham, S. N. Olof, H. Bayley, Light-activated communication in synthetic tissues. *Sci. Adv.* **2**, e1600056 (2016).
24. R. J. R. W. Peters *et al*., Multicompartment cascade reactions cascade reactions in multicompartmentalized polymersomes. *Angew. Chem. Int. Ed.* **53**, 146–150 (2014).
25. J. W. Hindley *et al*., Light-triggered enzymatic reactions in nested vesicle reactors. *Nat. Commun.* **9**, 1093 (2018).
26. E. Altamura *et al*., Highly oriented photosynthetic reaction centers generate a proton gradient in synthetic protocells. *Proc. Natl. Acad. Sci. U.S.A.* **114**, 3837–3842 (2017).
27. R. J. Brea *et al*., In situ reconstitution of the adenosine A2AReceptor in spontaneously formed synthetic liposomes. *J. Am. Chem. Soc.* **139**, 3607–3610 (2017).
28. K. Bernitzki, T. Schrader, Entirely artificial signal transduction with a primary messenger. *Angew. Chem. Int. Ed.* **48**, 8001–8005 (2009).
29. A. V. Pinheiro, D. Han, W. M. Shih, H. Yan, Challenges and opportunities for structural DNA nanotechnology. *Nat. Nanotechnol.* **6**, 763–772 (2011).
30. Y. Amir *et al*., Universal computing by DNA origami robots in a living animal. *Nat. Nanotechnol.* **9**, 353–357 (2014).
31. K. Charalambous *et al*., Engineering de novo membrane-mediated protein-protein communication networks. *J. Am. Chem. Soc.* **134**, 5746–5749 (2012).
32. E. A. Dennis, J. Cao, Y. H. Hsu, V. Magrioti, G. Kokotos, Phospholipase A2 enzymes: Physical structure, biological function, disease implication, chemical inhibition, and therapeutic intervention. *Chem. Rev.* **111**, 6130–6185 (2011).
33. J. Gullingsrud, K. Schulten, Lipid bilayer pressure profiles and mechanosensitive channel gating. *Biophys. J.* **86**, 3496–3509 (2004).
34. E. Perozo, D. M. Cortes, P. Sompornpisut, A. Kloda, B. Martinac, Open channel structure of MscL and the gating mechanism of mechanosensitive channels. *Nature* **418**, 942–948 (2002).
35. N. Mukherjee *et al*., The activation mode of the mechanosensitive ion channel, MscL, by lysophosphatidylcholine differs from tension-induced gating. *FASEB J.* **28**, 4292–4302 (2014).
36. B. Corry *et al*., An improved open-channel structure of MscL determined from FRET confocal microscopy and simulation. *J. Gen. Physiol.* **136**, 483–494 (2010).
37. G. van den Bogaart, V. Krasnikov, B. Poolman, Dual-color fluorescence-burst analysis to probe protein efflux through the mechanosensitive channel MscL. *Biophys. J.* **92**, 1233–1240 (2007).
38. J. L. Rigaud, B. Pitard, D. Levy, Reconstitution of membrane proteins into liposomes: Application to energy-transducing membrane proteins. *Biochim. Biophys. Acta.* **1231**, 223–246 (1995).
39. S. Pautot, B. J. Frisken, D. A. Weitz, Production of unilamellar vesicles using an inverted emulsion. *Langmuir* **19**, 2870–2879 (2003).
40. L. Song *et al*., Structure of staphylococcal alpha-hemolysin, a heptameric transmembrane pore. *Science* **274**, 1859–1866 (1996).
41. S. A. Walker, M. T. Kennedy, J. A. Zasadzinski, Encapsulation of bilayer vesicles by self-assembly. *Nature* **387**, 61–64 (1997).
42. Y. Elani *et al*., Constructing vesicle-based artificial cells with embedded living cells as organelle-like modules. *Sci. Rep.* **8**, 1–8 (2018).
43. S. Fujii, T. Matsuura, T. Sunami, Y. Kazuta, T. Yomo, In vitro evolution of α-hemolysin using a liposome display. *Proc. Natl. Acad. Sci. U.S.A.* **110**, 16796–16801 (2013).
44. G. A. Venkatesan *et al*., Adsorption kinetics dictate monolayer self-assembly for both lipid-in and lipid-out approaches to droplet interface bilayer formation. *Langmuir* **31**, 12883–12893 (2015).
45. O. G. Mouritsen *et al*., Activation of interfacial enzymes at membrane surfaces. *J. Phys. Condens. Matter* **18**, S1293–S1304 (2006).
46. P. Meers, K. Hong, D. Papahadjopoulos, Free fatty acid enhancement of cation-induced fusion of liposomes: Synergism with synexin and other promoters of vesicle aggregation. *Biochemistry* **27**, 6784–6794 (1988).
47. A. Melcrová *et al*., The complex nature of calcium cation interactions with phospholipid bilayers. *Sci. Rep.* **6**, 38035 (2016).
48. Y. V. Griko, Energetics of Ca2+–EDTA interactions: Calorimetric study. *Biophys. Chem.* **79**, 117–127 (1999).
49. H. Bading, D. D. Ginty, M. E. Greenberg, Regulation of gene expression in hippocampal neurons by distinct calcium signaling pathways. *Science* **260**, 181–186 (1993).